New Phytologist

Research

First cloning and characterization of two functional aquaporin genes from an arbuscular mycorrhizal fungus *Glomus intraradices*

Tao Li[1], Ya-Jun Hu[1], Zhi-Peng Hao[1], Hong Li[1], You-Shan Wang[2] and Bao-Dong Chen[1]

[1]State Key Laboratory of Urban and Regional Ecology, Research Center for Eco-Environmental Sciences, Chinese Academy of Sciences, Beijing, 100085, China; [2]Institute of Plant Nutrition and Resources, Beijing Academy of Agriculture and Forestry Sciences, Beijing, 100097, China

Author for correspondence:
Bao-Dong Chen
Tel: +86 10 62849068
Email: bdchen@rcees.ac.cn

Received: *7 August 2012*
Accepted: *22 September 2012*

New Phytologist (2013) **197:** 617–630
doi: 10.1111/nph.12011

Key words: aquaporin, arbuscular mycorrhizal (AM), drought tolerance, *Glomus intraradices*, heterologous expression, osmotic stress.

Summary

• Arbuscular mycorrhizal (AM) symbiosis is known to stimulate plant drought tolerance. However, the molecular basis for the direct involvement of AM fungi (AMF) in plant water relations has not been established.

• Two full-length aquaporin genes, namely *GintAQPF1* and *GintAQPF2*, were cloned by rapid amplification of cDNA 5′- and 3′-ends from an AMF, *Glomus intraradices*. Aquaporin localization, activities and water permeability were examined by heterologous expression in yeast. Gene expression during symbiosis was also analyzed by quantitative real-time polymerase chain reaction.

• GintAQPF1 was localized to the plasma membrane of yeast, whereas GintAQPF2 was localized to both plasma and intracellular membranes. Transformed yeast cells exhibited a significant decrease in cell volume on hyperosmotic shock and faster protoplast bursting on hypoosmotic shock. Polyethylene glycol (PEG) stimulated, but glycerol inhibited, the aquaporin activities. Furthermore, the expression of the two genes in arbuscule-enriched cortical cells and extraradical mycelia of maize roots was also enhanced significantly under drought stress.

• *GintAQPF1* and *GintAQPF2* are the first two functional aquaporin genes from AMF reported to date. Our data strongly support potential water transport via AMF to host plants, which leads to a better understanding of the important role of AMF in plant drought tolerance.

Introduction

Drought is a worldwide environmental problem which is becoming increasingly important in (semi-)arid areas under global climate changes (Querejeta *et al.*, 2009; Compant *et al.*, 2010). Drought stress exerts detrimental effects on plant growth, influences agricultural production and causes ecosystem degradation (Compant *et al.*, 2010). Plants can adapt themselves to drought stress by means of physiological responses regulated by gene expression (Ito *et al.*, 2006). Moreover, the arbuscular mycorrhizal (AM) symbiosis, a ubiquitous symbiotic association established between AM fungi (AMF) and roots of higher plants, which can be found in most terrestrial ecosystems, can also help plants to survive drought stress (Compant *et al.*, 2010). It has been demonstrated that AMF can protect host plants against drought stress by altering water flow into and out of the plants through hyphal networks, improving nutrient uptake and photosynthesis and promoting plant metabolic activities, such as the synthesis of abscisic acid (ABA) and proline (Augé, 2001; Ruiz-Lozano, 2003; Herrera-Medina *et al.*, 2007; Jahromi *et al.*, 2008; Ruíz-Sánchez *et al.*, 2011). The underlying mechanisms for the above-mentioned mycorrhizal functions may involve the regulation of the expression of drought-related genes in host plants, including aquaporin genes (Porcel *et al.*, 2006), *p5cs* genes encoding a rate-limiting enzyme in the biosynthesis of proline (Porcel *et al.*, 2004) and *nced* genes encoding a key enzyme in the biosynthesis of ABA (Aroca *et al.*, 2008). Moreover, extraradical mycelia of mycorrhizal fungi may uptake and transport water directly to host plants from the soil and even from space far from the root tips to alleviate plant water deficit (Allen, 2007; Egerton-Warburton *et al.*, 2007; Finlay, 2008). However, there are still arguments with regard to the significance of the contribution of AMF to the water uptake of host plants, and the molecular basis for the direct involvement of AMF in plant drought tolerance has not been established to date.

Water balances in plants are always accompanied by water movements across biological membranes by means of diffusion or through water channels (Ruiz-Lozano *et al.*, 2009). The capacity of water permeation mediated by water channels, known as aquaporins, is 10–100 times higher than that by diffusion (Agre *et al.*, 2002). Obviously, it is especially important to understand the key role of aquaporins in the mycorrhizal regulation of plant water relations. As a multifunctional protein family branched from the major intrinsic protein (MIP) superfamily, aquaporins are commonly present in nearly all organisms, facilitating the transport of certain small molecules in addition to water across

biological membranes, and are beneficial to the osmoregulation of organisms (Agre *et al.*, 2002; King *et al.*, 2004; Pettersson *et al.*, 2005; Tanghe *et al.*, 2006; Maurel *et al.*, 2008). Another mechanism in the osmoregulation of organisms through aquaporins is that, as part of a complex, they may be involved in intracellular Ca^{2+} signaling in response to osmotic stress (Benfenati *et al.*, 2011). In plants, aquaporins are classified into seven branches: plasma membrane intrinsic proteins (PIPs), tonoplast intrinsic proteins (TIPs), NOD26-like intrinsic proteins (NIPs), small basic intrinsic proteins (SIPs), GlpF-like intrinsic proteins (GIPs) and the recently identified hybrid intrinsic proteins (HIPs) and X-intrinsic proteins (XIPs) (Danielson & Johanson, 2008). As one of the strategies of AMF in helping host plants to survive drought stress, they can indirectly regulate plant aquaporin activities to influence plant water status (Maurel *et al.*, 2008). AMF may up-regulate or down-regulate plant aquaporin genes in leaves or roots to increase root hydraulic conductivity and leaf water potential and decrease leaf transpiration rate (Ruiz-Lozano *et al.*, 2006, 2009; Aroca *et al.*, 2008). The functions of aquaporin genes have been verified by means of gene overexpression or silencing (Yu *et al.*, 2005; Peng *et al.*, 2007; Sade *et al.*, 2009). Overall, the regulation by AMF of the expression of plant aquaporin genes under drought stress improves plant water status and drought tolerance (Aroca & Ruiz-Lozano, 2009).

There are five groups of fungal aquaporins, subdivided into two groups of classical aquaporins and three groups of aquaglyceroporins. These aquaporins have been fully described in *Saccharomyces cerevisiae* and filamentous fungi, but not in the symbiotic mycorrhizal fungi (Laizé *et al.*, 2000; Oliveira *et al.*, 2003; Pettersson *et al.*, 2005). It has been demonstrated that three aquaporins from an ectomycorrhizal fungus, the basidiomycete *Laccaria bicolor*, are responsible for water uptake and water exchange between host plants and ectomycorrhizal fungi (Dietz *et al.*, 2011). Most recently, Aroca *et al.* (2009) cloned the first AM fungal aquaporin gene (*GintAQP1*) from *Glomus intraradices*. Unfortunately, the aquaporin did not transport water when heterologously expressed in *Xenopus laevis* oocytes. Cloning of other aquaporin genes from AMF and the characterization of their activities would be particularly important to understand the molecular basis of AMF involvement in plant drought tolerance. Moreover, there are bidirectional water flows through aquaporins, and the direction of water flow follows the osmotic gradient (Allen, 2009). When AMF are exposed to drought stress, the lower osmotic potential in AMF is of key importance to their survival and uptake of water from soil. A better knowledge of AM fungal aquaporins would also definitely lead to a better understanding of the adaptation mechanisms of AMF themselves to drought stress.

In this study, we cloned two putative aquaporin genes from an AMF, *G. intraradices*, namely *GintAQPF1* and *GintAQPF2*. The localizations, functions and activities of the two aquaporin genes were verified by heterologous expression in *Pichia pastoris*, and the *in situ* detection of net Ca^{2+} and H^+ flux across transformed *P. pastoris* cells. Furthermore, the expression of *GintAQPF1* and *GintAQPF2* in colonized maize roots, cortical cells containing arbuscules and extraradical mycelia was also evaluated by quantitative real-time polymerase chain reaction (qRT-PCR). The study was aimed at the determination of the molecular basis of water uptake and water transfer to host plants by AMF, and also the drought tolerance of AMF themselves.

Materials and Methods

Preparation of biological materials

The AMF, *G. intraradices* Schenck & Smith (recently renamed as *Rhizophagus irregularis* by Krüger *et al.*, 2011), isolate AH01, was obtained from Beijing Academy of Agriculture and Forestry Sciences, China. The inoculum consisted of sand, spores, mycelia and colonized root fragments. For the cloning of AM fungal aquaporin genes, we first cultivated *G. intraradices* in association with host plants to obtain fungal materials. The growth medium was a 4 : 9 (w : w) mixture of sand and soil collected from Duolun (42° 02′N, 116°17′E), Inner Mongolia, China (hereinafter, 'soil' is used to refer to this substrate). The soil was autoclaved at 121°C for 1 h on two consecutive days. Before sowing, basal nutrients with 25 mg kg^{-1} Pi, 120 mg kg^{-1} K and 90 mg kg^{-1} N were carefully mixed into the soil (< 2 mm), together with 30 g of inoculum (*c.* 1800 spores) per pot. For the uninoculated controls, equivalent sterilized inoculum was mixed with the soil, together with a 5-ml filtrate of the AM inoculum to ensure the same microbial populations (except for AM propagules) in different inoculation treatments. The soil had a pH of 8.17 (1 : 2.5 soil to water) and an extractable Pi (with 0.5 M $NaHCO_3$) content of 6.73 mg kg^{-1}. Four seeds of *Sorghum vulgare* × *S. sudanense* and *Medicago sativa* were sown per pot. The experiment was conducted in a controlled-environment glasshouse at 14 h : 10 h and 25°C : 20°C (light : dark), 60% relative humidity. Deionized water was added as required to maintain 15% moisture content by regular weighing. At harvest (2 months after planting), plant roots were removed. The growth medium containing extraradical mycelia was carefully mixed before storage at −80°C in a refrigerator.

For the analysis of gene expression in extraradical mycelia, colonized roots and cortical cells containing arbuscules, maize (*Zea mays* L.) 'B73' was adopted as the host plant. The growth medium was the same as described previously. Before sowing, basal nutrients with 25 mg kg^{-1} Pi, 120 mg kg^{-1} K and 90 mg kg^{-1} N were mixed into the soil, together with 20 g of inoculum (*c.* 1200 spores) per pot of *G. intraradices* AH01, whereas, for the uninoculated controls, an extra 55 mg kg^{-1} Pi was added to the medium in order to reach similar plant Pi concentration and biomass as that of the inoculated treatments. Maize plants were grown in nylon mesh bags filled with 100 g of sterilized soil (< 2 mm); the bags were placed in the middle of plastic pots, and 200 g of sterilized soil was filled into the pot outside the nylon bags. The nylon mesh with a size of 37 μm prevented roots from growing into the outer compartment, but allowed access to extraradical mycelia to this so-called 'hyphal compartment' (HC). Only one plant was grown in each pot. There were 10 replicates of each inoculation treatment, giving a total of 20 pots, which were set up in a randomized block design. For the realization of two water regimes, half of the pots (both

inoculated and uninoculated) were maintained under well-watered conditions (12% water content) throughout the experiment and the other half were subjected to drought stress, in which the soil water content was maintained at 6% for 10 d before harvest. The experiment was conducted in a controlled growth chamber at a light intensity of 700 μmol m^{-2} s^{-1}, 16 h : 8 h and 25°C : 20°C (light : dark), 70% relative humidity. Deionized water was added as required to maintain the moisture content by regular weighing. At harvest (42 d after planting), shoots and roots were separated and the roots were carefully cleaned with tap water. One gram of roots was stored at −80°C. The relative water content was determined according to Ruiz-Lozano & Azcon (1997). The percentage of mycorrhizal root infection in maize was estimated by visual observation of fungal colonization after roots had been immersed in 10% KOH, cleaned with deionized water and stained with 0.05% trypan blue in lactic acid (v : v) (Phillips & Hayman, 1970). The extent of mycorrhizal colonization was calculated according to the root segment frequency ordinary method (Biermann & Linderman, 1981).The soil from HC was collected and mixed; 10 g was frozen in liquid nitrogen and stored at −80°C until RNA extraction. Another 4 g of soil from HC was used to measure the hyphal length density by a grid-line intercept technique (Jakobsen *et al.*, 1992).

Cloning of *G. intraradices* aquaporin genes

One gram of growth medium from the first experiment was taken, and total RNA and genomic DNA were extracted using TRIZOL (Invitrogen, Grand Island, New York, USA) and a FastDNA® SPIN Kit for Soil (MP Biomedicals, Solon, Ohio, USA), respectively. In order to purify the total RNA, an RNeasy Plant Mini Kit (Qiagen, Santa Clarita, CA, USA) was used following the manufacturer's instructions. cDNA was synthesized from the RNA samples using a PrimeScript® RT Reagent Kit (TAKARA Biotechnology Co. Ltd, Dalian, China). Synthesized cDNA was amplified and the products were separated in 1% agarose gel. The bands (*c.* 550 and 450 bp) were cut, eluted with a QIAquick gel extraction kit (Qiagen, USA) and cloned into pGEM-T Easy vector (Promega Corp., Madison, Wisconsin, USA). The vectors with inserted target fragments were transformed into *Escherichia coli* JM 109-competent cells (TAKARA Biotechnology Co. Ltd), followed by sequencing of the purified plasmid DNA.

The rapid amplification of cDNA ends (RACE) technique was applied to determine the full-length sequence based on the obtained cDNA using the 5′-RACE system (Version 2.0, Invitrogen) and 3′-Full RACE Core Set (Version 2.0, TAKARA Biotechnology Co. Ltd; Table 1). After 5′- and 3′-RACE, PCR was performed with high-fidelity KOD FX (TOYOBO Life Science, Osaka, Japan), using the primers, full *GintAQPF1* and full *GintAQPF2* (Table 1), to obtain the full-length gene.

Sequence comparisons and protein translation were conducted using the Basic Local Alignment Search Tool (BLAST) (Altschul *et al.*, 1990) and the translation tool at the ExPASy Molecular Biology Server (http://web.expasy.org/translate), respectively. The alignment of *GintAQPF1* and *GintAQPF2* with other fungal aquaporins, plus *E. coli* AqpZ (a classical aquaporin; Calamita *et al.*, 1995) and *E. coli* GlpF (a well-known aquaglyceroporin; Heller *et al.*, 1980), was analyzed using ClustalW (a program in *MEGA* version 4). The phylogenetic tree was generated based on the neighbor-joining method using *MEGA* version 4 (Tamura *et al.*, 2007). The hypothetical transmembrane topology of *GintAQPF1* and *GintAQPF2* was predicted by the HMMTOP transmembrane topology prediction server (Gabor & Istvan, 2001).

Preparation of root sections for laser microdissection

According to Gomez *et al.* (2009), Steedman's wax was prepared to embed maize root fragments (length, *c.* 1 cm). Transverse root sections (thickness, 14 μm) were obtained using a Leica RM 2016 rotary microtome (Leica Microsystems Incorporated, Nussloch, Germany) at 20°C. Sections were loaded onto a 1.4-μm RNase-free PEN membrane-covered slide with a steel frame (Leica, Germany). The contour of the cortical cells containing arbuscules was cut using a laser microdissection system (LMD 6000, Leica, Germany) and target cells were collected, depending on gravity, into the caps of RNase-free microcentrifuge tubes containing 100% ethanol. The harvested cells were frozen in liquid nitrogen, and stored at −80°C until RNA extraction. Five mature roots were randomly selected from each plant and, from each root fragment, *c.* 150 cells were cut by a laser for analysis.

Sterilization and germination of spores

One thousand spores were collected from the fungal inoculum and surface sterilized according to Bécard & Fortin (1988). After sterilization, every 300 spores were separately germinated on 0.8% (w : v) water agar at 27°C in the dark. One week later, after confirming spore germination microscopically, spores were harvested, frozen in liquid nitrogen and stored at −80°C.

Gene expression analysis

Gene expression analysis was performed by qRT-PCR in a Bio-Rad iQ5 Optical system (Bio-Rad, Hercules, CA, USA). The extractions of total RNA of colonized maize roots and of mycelia from the HC medium were carried out using TRIZOL and a FastRNA® pro Soil Direct Kit (MP Biomedicals), respectively, according to the manufacturer's instructions. The RNAs of cortical cells containing arbuscules and germinated spores were extracted using an RNeasy Plant Mini Kit. cDNA was synthesized as described previously. Twenty-five microliters of reaction medium contained 5 μl of 1 : 10-diluted cDNA samples, 400 nM gene-specific primers (RT *GintAQPF1* and RT *GintAQPF2*, Table 1) and 12.5 μl of SYBR Green I PCR Mix (TAKARA Biotechnology Co. Ltd). A control analysis was performed by adding each RNA sample or water instead of the cDNA sample to the reaction medium to avoid contamination by genomic DNA or to exclude the formation of a primer–dimer. The PCR program was as follows: one cycle at 95°C for 30 s, and 40 cycles of 5 s at 95°C, 45 s at 58°C and 30 s at 72°C. Data collection was performed at

Table 1 Polymerase chain reaction (PCR) primers used in this study

Primer		5′→3′
GintAQPF1-ID	Forward primer	GACTTGTTAACGATAACGTAC
	Reverse primer	CATTCCAATACCAAATGGAGC
GintAQPF2-ID	Forward primer	GGCTACTGCTCTATGCTCATG
	Reverse primer	GGACAAAAGAGATGTTATAGG
GintAQPF1-3race	Inner	TTGCAGATGGAGTTTCAGTAGC
	Outer	TGACTTGATTCAACCTGAAGC
GintAQPF2-3race	Inner	CACTTTCTTTATTGGTTA
	Outer	GCAGCTCGTGATTTTGGACC
GintAQPF1-5race	GSP1	GAGAAACCGAAACAGAATGG
	GSP2	CGGTAATGGTGAACCAGCTGC
	GSP3	GTAAGCGGTTCCAACAAACTCGC
GintAQPF2-5race	GSP1	TAACCAATAAAGAAAGTG
	GSP2	GGTCCAAAATCACGAGCTGC
	GSP3	CCGGTTTCAAACCCAAGTG
Full*GintAQPF1*	Forward primer	TCAAAATGCTAGATGCAGAAC
	Reverse primer	TTAGTTTTGGGATTCTATGTC
Full*GintAQPF2*	Forward primer	ATGGCGGATGAACGTGGACCG
	Reverse primer	CTAGGCTACTGCTCTATGCTC
RT*Gint18S rRNA*	Forward primer	TGTTAATAAAAATCGGTGCGTTGC
	Reverse primer	AAAACGCAAATGATCAACCGGAC
RT *GintAQPF1*	Forward primer	CATTTGGGCTCCAATCTCTGGAGG
	Reverse primer	CTCCATCTGCAAGTAAGGTTGCTG
RT *GintAQPF2*	Forward primer	GAACAAGAGGAGCACCAGCCACTG
	Reverse primer	CCACTAACTGCAATACCCAAAGCG
GintAQPF1-Y	Forward primer	CCGGAATTCTCAAAATGCTAGATGCAGAAC
	Reverse primer	CCGCTCGAGTTAGTTTTGGGATTCTATGTC
GintAQPF2-Y	Forward primer	CCGGAATTCATGGCGGATGAACGTGGACCG
	Reverse primer	CCGCTCGAGCTAGGCTACTGCTCTATGCTCATG
pGAP Forward- 3′ AOX1	Forward primer	GTCCCTATTTCAATCAATTGAA
	Reverse primer	GCAAATGGCATTCTGACATCC
GFP	Forward primer	CCGCTCGAGATGGGTAAAGGAGAAGAAC
	Reverse primer	ATAGTTTAGCGGCCGCTTAAGATCTGAGTCCGGACTTG
GintAQPF1-GFP-Y	Reverse primer	CCGCTCGAGGTTTTGGGATTCTATGTC
GintAQPF2-GFP-Y	Reverse primer	CCGCTCGAGGGCTACTGCTCTATGCTCATG

58°C. The melting curve was produced according to the following program: 10 s at 70°C, and heating to 100°C at a rate of 0.2° C s^{-1}, and data were continuously collected. The data were analyzed by the $2^{-\Delta\Delta Ct}$ method (Pfaffl, 2001). *Gint18S rRNA* (Gónzalez-Guerrero *et al.*, 2005) was used as reference. The similarity of the amplified fragment of *Gint18S rRNA* between *G. intraradices* AH01 and *G. intraradices* DAOM 197198 was 100%, which was confirmed by sequencing. qRT-PCR was conducted in triplicate using at least three independent cDNAs.

Heterologous expression of *G. intraradices* aquaporin genes in yeast

The open reading frames of *G. intraradices* aquaporins were amplified by PCR using the primers *GintAQPF1*-Y and *GintAQPF2*-Y (containing *EcoR*I and *Xho*I sites, Table 1). The PCR products were cloned into pGEM-T Easy vector, and the resulting vectors were transformed into *E. coli* JM 109-competent cells. The plasmid DNAs purified by restriction digestion with *EcoR*I and *Xho*I (Fermentas, Burlington, Ontario, Canada) were inserted into the *Pichia* expression vector pGAPZ B (Invitrogen, USA) cut by *EcoR*I and *Xho*I, respectively. The vector has been demonstrated to have high efficiency in the expression of recombinant proteins in *P. pastoris* (Waterham *et al.*, 1997). The resulting plasmids, pGAPZ B-*GintAQPF1* and pGAPZ B-*GintAQPF2*, were linearized by *Avr*II (New England Biolabs, Hitchin, Hertfordshire, UK) and transformed into *P. pastoris* GS115-competent cells (Invitrogen) by electroporation. As a control, the linearized pGAPZ B was transformed into yeast cells. Transformation, cell culture and isolation of putative multicopy

recombinants were performed according to the manufacturer's instructions. The pGAP Forward-3′ AOX1 primers (Table 1) were used to analyze and verify Zeocin™-resistant transformants.

Aquaporin localization in yeast was performed by fusing the C-terminus of GintAQPF1 or GintAQPF2 to a green fluorescent protein (GFP). Briefly, the open reading frames of aquaporins were amplified by PCR using the primers *GintAQPF1*-Y Forward and *GintAQPF1-GFP*-Y, and *GintAQPF2*-Y Forward and *GintAQPF2-GFP*-Y (containing *EcoR*I and *Xho*I sites; Table 1). The open reading frame of *GFP* was amplified by PCR using the primer *GFP* (containing *Xho*I and *Not*I sites) (Table 1) and plasmid pRSGFP-C1 (Clontech, Palo Alto, CA, USA) as a template. The DNAs purified by restriction digestion and pGAPZ B cut by *EcoR*I and *Not*I (New England Biolabs) were ligated by T4 DNA ligase (Promega Corp.). The resulting plasmids, pGAPZ B-*GintAQPF1-GFP* and pGAPZ B-*GintAQPF2-GFP*, were transformed into GS115 cells as described previously. Confocal microscopy and image capture were performed using a laser scanning confocal microscope (Leica DMI 6000B-CS, Germany). Images were converted to TIFF, and processed in Adobe® Photoshop® 7.0 (Adobe Systems Incorporated, San Jose, CA, USA).

Yeast cell volume was determined as described by Prudent *et al.* (2005). Transformed cells were pregrown in yeast extract peptone dextrose (YPD) medium. The hyperosmotic shock was realized by resuspending transformed cells in YPD medium containing 1 M sorbitol. As a control, transformed cells were resuspended in new YPD medium. The transformed cells under both treatments were grown to an optical density at 600 nm (OD_{600}) of 1.0. Cells were then loaded onto a slide and the projected area (S) of 20 cells was determined via an inverted phase contrast light microscope (Lumar V12, Leica, Germany) and Adobe® Photoshop® 7.0. The volume of cells was calculated using the formula $V = \frac{4}{3}\frac{S^{3/2}}{\sqrt{\pi}}$. Values are an average of three independent observations.

Water transport through protoplasts was measured according to Pettersson *et al.* (2006). Transformed cells were grown to an OD_{600} of 1.2 and harvested at room temperature. The cells were washed once in water and then in 1 M sorbitol, and resuspended in SCE buffer (1 M sorbitol, 0.1 M sodium citrate, 10 mM EDTA, 0.2 mM β-mercaptoethanol, pH 6.8). The protoplasts were prepared by the addition of 2000 U lyticase (Sigma, Ronkonkoma, New York, USA) per milliliter of yeast culture medium in SCE buffer and incubation of the cells at 30°C for 4 h. The protoplasts confirmed by light microscopy were harvested, washed twice and resuspended in STC buffer (1 M sorbitol, 10 mM Tris–HCl, pH 7.5, 10 mM $CaCl_2$). Protoplast bursting on hypo-osmotic shock was realized by means of dilution of the STC buffer containing protoplasts to 0.5 M sorbitol with STC buffer free of sorbitol at $t = 0$. On hypo-osmotic shock, the amount of burst protoplasts increased which, in turn, caused a decrease in OD. OD_{600} was monitored every 5 s for 65 s. Each water transport assay was replicated three times.

For growth analysis of transformed cells under osmotic stress, overnight cultures of different transformed cells were adjusted to an OD_{600} of 0.2 in YPD containing 100 μg ml^{-1} Zeocin™. Fifty microliters of each were taken and added to 10 ml YPD containing a final concentration of 25% polyethylene glycol 6000 (PEG6000) or 1 M glycerol or no exogenous osmolytes. The cells were incubated at 30°C in a shaking incubator (200 rpm) for 30 h, during which samples were taken at 9, 12, 15, 18, 21 and 30 h. For glycerol and PEG treatments, 500 μl medium was sampled with resuspension in 500 μl YPD twice at each sampling time to avoid the effects of osmolytes. The changes in cell density were monitored by OD_{600} using Microplate Reader Spectra (SPECTRA max190, Molecular Devices, San Francisco, CA, USA). Each growth assay was replicated independently three times.

Measurement of extracellular Ca^{2+} influx and intracellular H^+ efflux in response to glycerol and PEG6000 treatments

Net Ca^{2+} and H^+ fluxes were measured using the noninvasive scanning ion-selective microelectrode (ion flux measurement, MIFE), as described by Shabala *et al.* (2001, 2006). Transformed yeast cells were grown to an OD_{600} of unity in YPD containing a final concentration of 25% PEG6000 or 1 M glycerol or no exogenous osmolytes. Ten microliters of transformed cells were immobilized on a coverslip for 5 min, washed off with standard medium to ensure a monolayer of attached cells and incubated in the standard medium for 5 min. The composition (in mM) of the standard medium was as follows: $CaCl_2$, 0.1; KCl, 0.1; Mes, 0.3; glucose, 10; pH adjusted to 6.0. Microelectrodes were positioned 10 μm above the attached cell population consisting of 15 cells with equal size. Ion concentration was measured at two excursion points, one 10 μm above the cell population and the other 20 μm away, at a frequency of 0.05 Hz manipulated by a computer. Ion concentrations could be converted into ion fluxes. The kinetics of net Ca^{2+} and H^+ fluxes near each cell population were monitored for 10 min. For each sample, four clones were incubated in 10 ml YPD, and the resulting four cell populations were measured. The data obtained were analyzed and converted into Ca^{2+} influx (negative) and H^+ efflux (positive) (pmol cm^{-2} s^{-1}) using the MageFlux program (http://www.xuyue.net/mageflux). The ion flux assay around each type of transformed cells was replicated independently three times.

Statistical analysis

Data were expressed as the mean ± SD of observations from independent experiments. One-way ANOVA was performed for data from the Ca^{2+} or H^+ flux experiments and for the cell volume measurements, whereas two-way ANOVA was performed for data on the root relative water content, root colonization and hyphal length density, using SPSS (Version 13.0, SPSS Inc., Chicago, IL, USA) to test for the significance of treatment effects. Following ANOVA, Duncan's multiple-range test (Duncan, 1955) was performed to make comparisons between treatments. Data from the maize experiment were subjected to t-test in Microsoft® Excel 2003 to compare the two water regimes. For curve fitting of yeast growth in the heterologous gene expression experiment, nonlinear regression and curve comparison by sum-

of-squares *F* test were performed using Origin 8.6.0 (32-bit) Sr2b98 (OriginLab Corporation, Wellesley, Massachusetts, USA; http://www.OriginLab.com).

Results

Cloning of aquaporin genes and *in silico* protein analyses

Based on two conserved asparagine–proline–alanine (NPA) motifs located in aquaporins, we used tblastn in the *G. intraradices* expressed sequence tag (EST) database in the National Center for Biotechnology Information (NCBI) (http://www.ncbi.nlm.nih.gov), screened out a total of 70 sequences and found five candidate genes by pseudogene examination. Only two qualified sequences (gi: 282304637 and gi: 282307341) were obtained and successfully identified by PCR amplification (primers: *GintAQPF1*-ID and *GintAQPF2*-ID, Table 1) and sequencing. By 5′-RACE and 3′-RACE techniques, we cloned the full-length cDNA sequences of two *G. intraradices* aquaporins and named them *GintAQPF1* and *GintAQPF2* (GenBank accession numbers JQ412059 and JQ412060) based on the obtained cDNA. A control experiment was conducted by PCR amplification with specific primers (Table 1) from the genomic DNA extracted from noninoculated roots and medium without the inoculum. No visible PCR products in the controls confirmed the AM fungal origin of the two genes. We also screened 25 906 nonredundant virtual transcripts (NRVTs) of *G. intraradices* (DAOM 197198) according to Tisserant *et al.* (2012), and only two predicted aquaporin genes (step3_c3477 and step3_c435) were found. The similarities between *GintAQPF1* and step3_c3477, and between *GintAQPF2* and step3_c435, were 94% and 98%, respectively.

GintAQPF1 is 1093 bp long and contains three introns, the open reading frame of which consists of 831 bp corresponding to 276 amino acids (Fig. 1a); *GintAQPF2* does not contain any introns, and the coding region comprises 951 bp corresponding to 316 amino acids (Fig. 1b).

GintAQPF1 contains asparagine–proline–lysine (NPK) and NPA motifs (in red, Fig. 1a) as part of the pore constriction in aquaporin, whereas GintAQPF2 contains NPA and asparagine–alanine–alanine (NAA) motifs (in red, Fig. 1b). Both had six transmembrane domains as in all other aquaporins (Fig. 1) (Pettersson *et al.*, 2005). The other major constriction at the center of the pore was called the aromatic/arginine (ar/R) region, which is narrower than the NPA region, and is responsible for pore selectivity depending on the pore diameter (Beitz, 2005). Comparing the cloned aquaporin genes with two model aquaporins, water-specific aquaporin 1 (AQP1) and the *E. coli* glycerol-porin GlpF (Ian & Daniel, 2004), we found that only position F58 (aromatic amino acid) was conserved in GintAQPF1 according to AQP1, and only position F200 was conserved in GintAQPF2 according to GlpF. In addition, we used the Calmodulin Target Database to predict the putative calmodulin binding sites. GintAQPF1 had a calmodulin binding site in the N-terminus, whereas there was no calmodulin binding site in GintAQPF2.

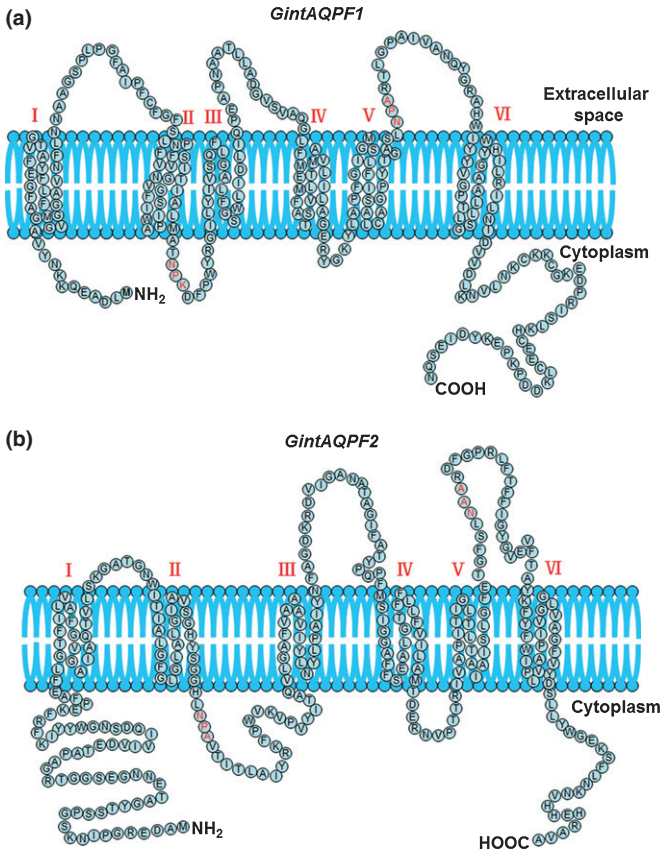

Fig. 1 Predicting the topology of (a) GintAQPF1 (831 bp corresponding to 276 amino acids) and (b) GintAQPF2 (951 bp corresponding to 316 amino acids).

Phylogenetic analysis of aquaporins

The deduced *G. intraradices* aquaporins were compared with other fungal aquaporins, including GintAQP1 (Aroca *et al.*, 2009), aquaporins of *L. bicolor* (Dietz *et al.*, 2011) and fungal XIPs (Gupta & Sankararamakrishnan, 2009). *Escherichia coli* AqpZ and *E. coli* GlpF were also taken into account because of their well-known functions. Three main branches could be distinguished (Fig. 2). GintAQPF1 and the first *G. intraradices* aquaporin GintAQP1 were classified into classical aquaporins, water-specific channel, which also included one *L. bicolor* (*L. bicolor*, XP001885271) homolog. We named the second branch as aquaglyceroporins, comprising GintAQPF2 and three other *L. bicolor* homologs (*L. bicolor,* XP001878806; XP001878999; XP001884805), which were identified as aquaglyceroporins by Dietz *et al.* (2011), because GlpF was defined as a well-known aquaglyceroporin. Fungal XIPs were classified into the third branch, where no *G. intraradices* aquaporins were found.

Localization of GintAQPF1 and GintAQPF2 in yeast

Aquaporin localization in yeast cells was performed using confocal microscopy by fusing their C-termini to GFP. GintAQPF1 was localized to the plasma membrane of yeast cells (Fig. 3), whereas GintAQPF2 showed a clear localization to the plasma membrane (Fig. 3b) and intracellular membranes (Fig. 3a).

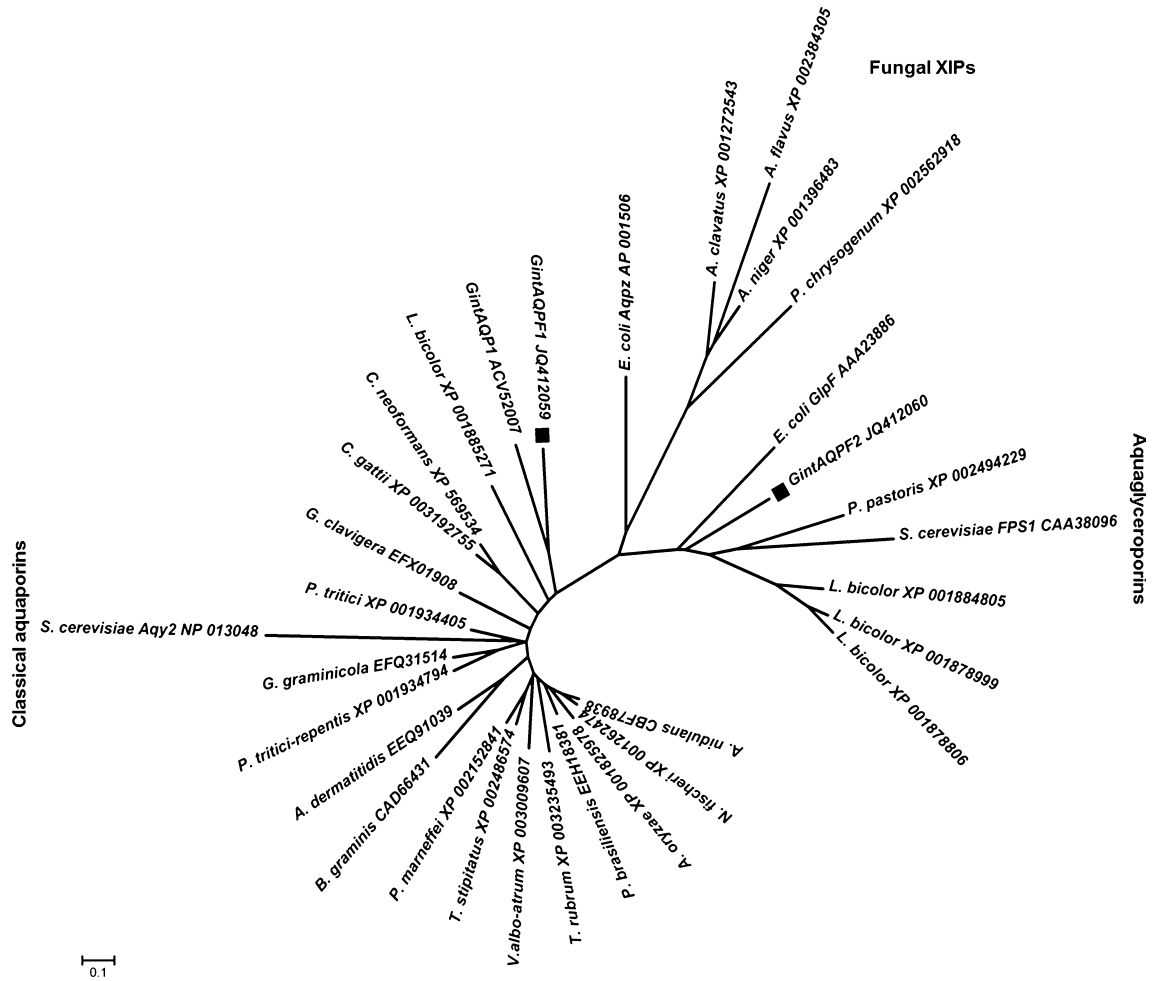

Fig. 2 Phylogenetic tree of GintAQPF1, GintAQPF2 and other fungal aquaporins based on the neighbor-joining method. The accession numbers are shown after the species names. GintAQPF1 and GintAQPF2 are labeled using a black square.

Water transport assay

Water transport through GintAQPF1 and GintAQPF2 was manifested by the determination of the cell volume on hyperosmotic shock and protoplast bursting on hypo-osmotic shock. Overexpression of *GintAQPF*1 and *GintAQPF*2 led to a significant decrease in cell volume in response to 1 M sorbitol, compared with that of empty vector-transformed cells (Fig. 4). There was no significant difference in cell volume between *GintAQPF*1- and *GintAQPF*2-transformed yeast cells. Water flux across the plasma membrane of protoplasts mediated by GintAQPF1 and GintAQPF2 was also dynamically monitored by measuring OD_{600} on hypo-osmotic shock. *GintAQPF*1- and *GintAQPF*2-transformed protoplasts burst more rapidly than those transformed with empty vector, and *GintAQPF*2-transformed protoplasts burst more rapidly than those of *GintAQPF*1 (Fig. 5).

Growth of transformed yeast overexpressing the aquaporin genes

The gene functions were analyzed by monitoring the growth of transformed cells in response to osmotic stress. Curve-fitting

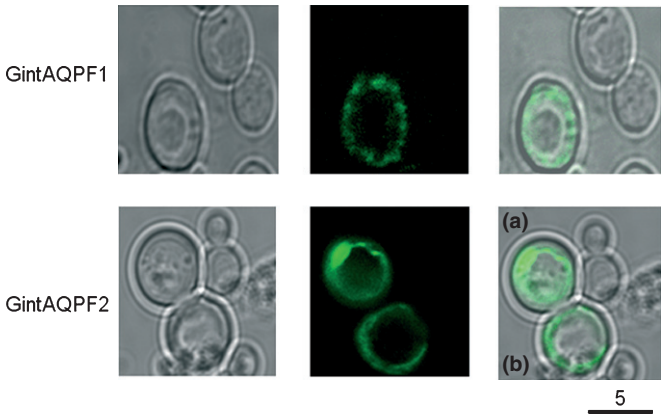

Fig. 3 Localization of GintAQPF1 (upper) and GintAQPF2 (lower) in *Pichia pastoris* GS115. GintAQPF1 was localized to the plasma membrane, whereas GintAQPF2 was found in both the plasma membrane (b) and intracellular membranes (a). Images from left to right show bright field, green fluorescent protein (GFP) fluorescence and overlay of bright field and GFP, respectively. Bar, 5 μm.

analysis showed that the overexpression of *GintAQPF*1 and *GintAQPF*2 resulted in a significant decrease in OD_{600} of transformed cells in response to 1 M glycerol, compared with the

control cells into which pGAPZ B (empty vector) was transformed (Fig. 6a). GintAQPF2 was more sensitive than GintAQPF1 to glycerol. Overexpression of *GintAQPF*1 and *GintAQPF*2 increased significantly the cell survival rate, compared with control cells under PEG stress. When comparing GintAQPF1 with GintAQPF2, there was no significant difference in the alleviation of PEG stress (Fig. 6b). In order to exclude the growth difference caused by different plasmids, we monitored the growth of the three types of transformed cells in YPD without exogenous osmolytes. The results showed that there was no significant difference in growth among the transformed cells (Fig. 6c). The data confirmed that growth changes of the transformed cells in response to glycerol and PEG were derived from genes inserted in the plasmids.

Gene expression in colonized maize roots and extraradical mycelium

At 42 d after planting of maize plants, the roots, shoots and medium in HC were collected. There was no significant difference in plant dry weight and Pi concentration between inoculated and noninoculated treatments under drought stress (data not shown). Drought increased the root colonization and stimulated significantly hyphal development (Table 2). *Glomus intraradices* increased significantly the root relative water content compared with that of uninoculated treatments under drought stress (Table 2).

Gene expression analysis was first performed by qRT-PCR for different fungal structures. Both *GintAQPF1* and *GintAQPF2* were highly expressed in arbuscule-enriched cortical cells. There was lowest expression of the two genes in germinated spores (Fig. 7).

For colonized maize roots and cortical cells containing arbuscules, drought stress up-regulated the expression of *GintAQPF1* and *GintAQPF2* (Figs 8, 9). In extraradical mycelium from HC, drought stress also stimulated significantly the expression of both genes (Fig. 10).

Ca^{2+} and H^+ flux from transformed yeast cells in response to osmotic treatments

Using the MIFE technique, we measured Ca^{2+} and H^+ fluxes across cell membranes. There was no significant difference in Ca^{2+} influx and H^+ efflux among the three types of transformed cells for the control treatment, or in H^+ efflux between *GintAQPF*1- and *GintAQPF*2-transformed cells for glycerol and PEG treatments (Fig. 11). In response to different osmotic treatments, GintAQPF1 and GintAQPF2 changed the signatures of Ca^{2+} and H^+ flux of transformed cells in comparison with control cells. GintAQPF1 and GintAQPF2 caused a decrease in Ca^{2+} influx into and H^+ efflux from transformed cells subjected to glycerol; however, when exposed to PEG, the two aquaporins caused an increase in Ca^{2+} influx and H^+ efflux (Fig. 11). It should be noted further that there were also differences in Ca^{2+} flux between *GintAQPF*1- and *GintAQPF*2-transformed cells in response to glycerol and PEG treatments. GintAQPF1 triggered a more profound increase in Ca^{2+} influx in contrast with that by GintAQPF2 (Fig. 11).

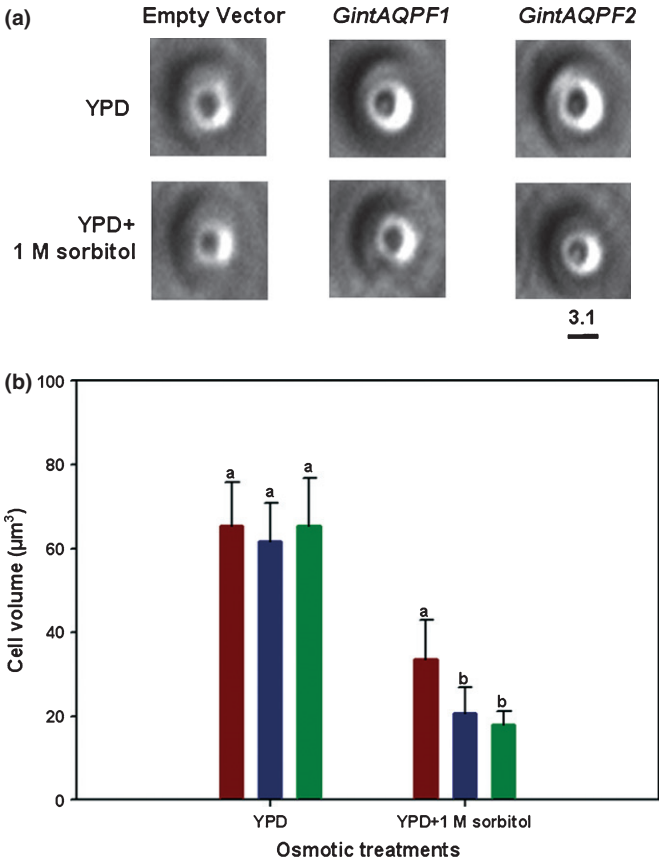

Fig. 4 Effects of hyperosmotic shock on (a) cellular morphology and (b) cell volume of *GintAQPF*1- and *GintAQPF*2-transformed yeast. Different letters above the columns indicate significant differences ($P < 0.05$) between different cell groups under the same osmotic treatment. Empty Vector, red bars; *GintAQPF*1, blue bars; *GintAQPF*2, green bars. The error bars represent SD. Bar, 3.1 μm.

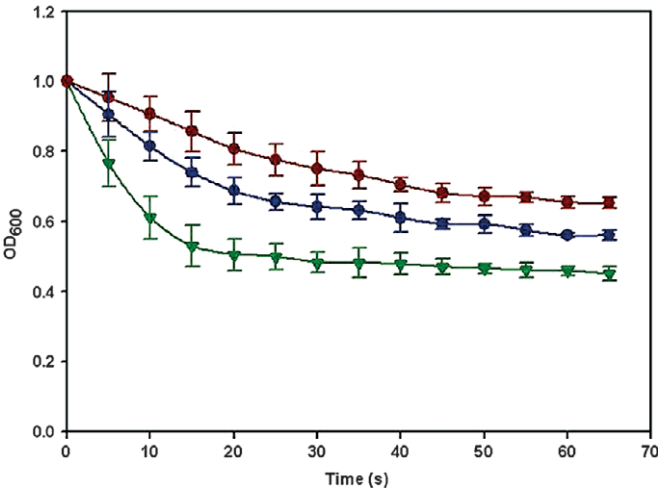

Fig. 5 Effects of *GintAQPF*1 and *GintAQPF*2 on protoplast bursting on hypo-osmotic shock. Empty Vector, red circles; *GintAQPF1*, blue circles; *GintAQPF2*, green triangles. OD_{600}, optical density at 600 nm. The error bars represent SD [correction added after online publication 19 November 2012: information describing the variables displayed in this figure is now included within the figure legend].

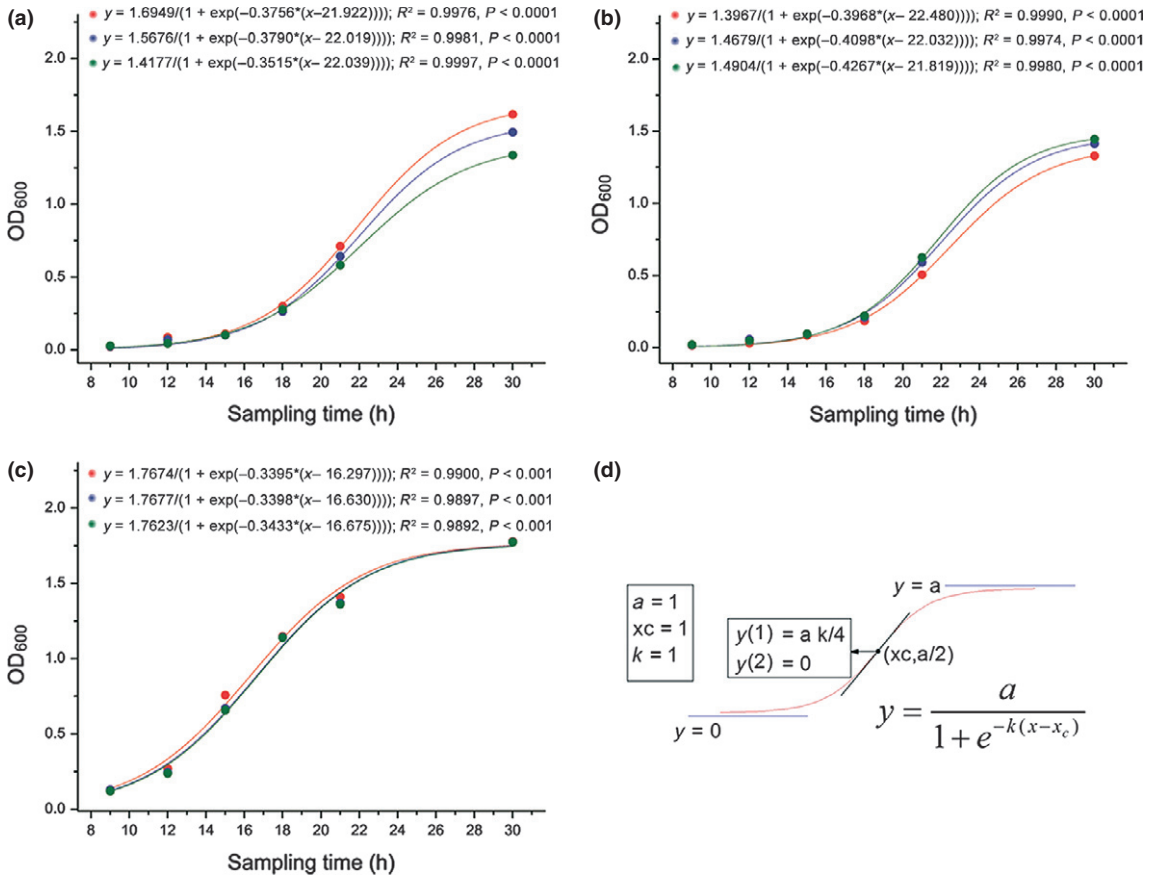

Fig. 6 Growth responses to osmotic stress of transformed yeast overexpressing *GintAQPF1* and *GintAQPF2*. Each data point represents the mean of the values from three independent experiments. Curve fitting by the Slogistic1 model, $y = a/\{1 + \exp[-k(x - x_c)]\}$, in Origin 8.6.0 Sr2b98 (OriginLab Corporation). Red, blue and green curves represent the growth curves of *Pichia pastoris* overexpressing Empty Vector, *GintAQPF1* and *GintAQPF2*, respectively. (a) *Pichia pastoris* Gs 115 in 1 M glycerol. There were significant differences ($P < 0.05$) in parameter '*a*' among the curves, but no significant differences among the curves for x_c and *k*. (b) *Pichia pastoris* Gs 115 in 25% polyethylene glycol (PEG). Parameter '*a*' was significantly different between *GintAQPF1*/*GintAQPF2* and Empty Vector ($P < 0.05$), but with no significant difference between *GintAQPF1* and *GintAQPF2*. No significant difference among curves for x_c and *k*. (c) *Pichia pastoris* Gs 115 under normal conditions. No significant differences among the curves for *a*, x_c and *k*. (d) Sample curve, formula and parameters (*a*, x_c and *k*) for curve fitting.

Discussion

It is well accepted that AM external hyphae can take up water directly by hydraulic lift or from soil micropores when roots are unable to access and redistribute water along hyphal networks, to facilitate plant water relations (Egerton-Warburton *et al.*, 2007; Allen, 2009). However, because of the absence of molecular evidence for water transport by hyphae, it is difficult to elucidate the basis of the water potential difference between soil and hyphae to guarantee water uptake and the maintenance of AM

Table 2 Mycorrhizal colonization, extraradical hyphal length density and root relative water content of maize plants under different water regimes

Soil water content (%)	Colonization rate (%)		Hyphal length density (m g^{-1} soil)		Relative water content of root (%)	
	Inoculated	Uninoculated	Inoculated	Uninoculated	Inoculated	Uninoculated
12	42a[1]	0a	1.69b	0c	78a	77a
6	48a	0a	1.94a	0c	77a	69b
Significance[2] of Water (W)	ns		*		*	
Inoculation (I)	**		**		*	
W × I	ns		*		*	

[1]Duncan's multiple-range test was performed across all treatments when interactions were significant, and *t*-test was performed to compare differences between water treatments under the same inoculation treatment when there were no significant interactions. Different letters following the means indicate significant differences ($P < 0.05$) between treatments.
[2]ANOVA output: *, $P < 0.05$; **, $P < 0.01$; ns, not significant.

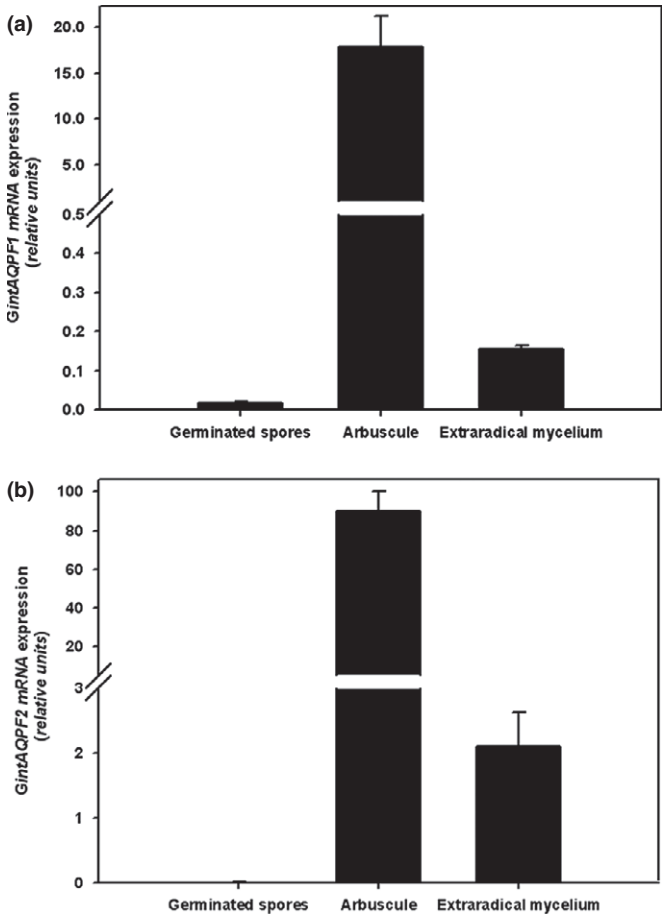

Fig. 7 Expression of aquaporin genes, *GintAQPF*1 (a) and *GintAQPF*2 (b), in germinated spores, cortical cells containing arbuscules and extraradical mycelium. The error bars represent SD.

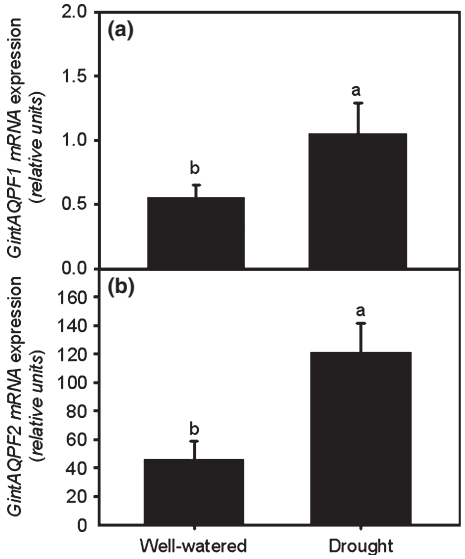

Fig. 8 Effects of drought stress on the expression of aquaporin genes, *GintAQPF*1 (a) and *GintAQPF*2 (b), in maize roots colonized by *Glomus intraradices*. The data were obtained on RNAs from whole roots. Different letters above the columns indicate significant differences (*t*-test, $P < 0.05$) between water treatments. The error bars represent SD.

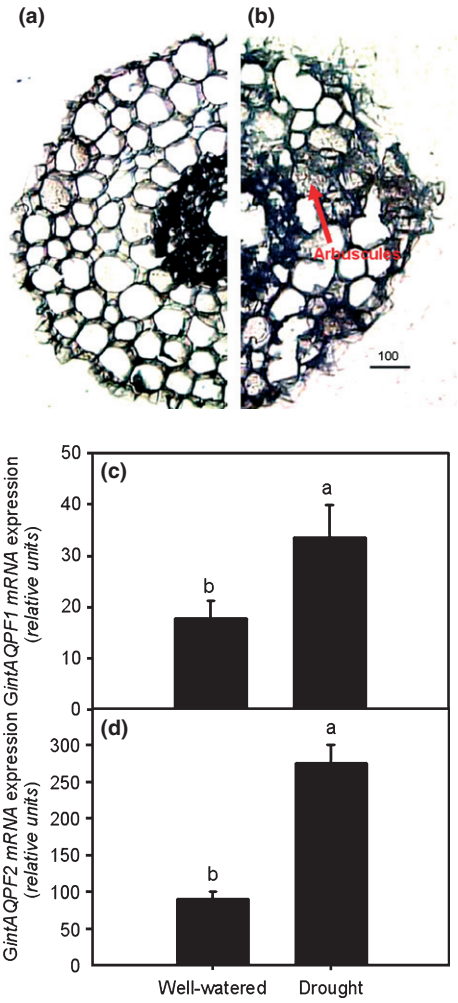

Fig. 9 Transverse root sections of maize plants inoculated without (a) and with (b) *Glomus intraradices*. The arrow indicates a cortical cell containing an arbuscule in mycorrhizal roots under drought stress. Bar, 100 μm. Effects of drought stress on the expression of aquaporin genes, *GintAQPF*1 (c) and *GintAQPF*2 (d), in cortical cells containing arbuscules. The data were obtained on RNAs from laser-microdissected arbuscules. Different letters above the columns indicate significant differences (*t*-test, $P < 0.05$) between water treatments. The error bars represent SD.

fungal growth under drought stress. In this study, we first cloned two functional aquaporin genes from *G. intraradices*, namely *GintAQPF1* and *GintAQPF2*. We revealed the coping strategies of the two aquaporins during osmotic stress by gene function verification and the detection of protein activities. The higher relative water content in the colonized roots and increased expression of the two genes in both root cortical cells containing arbuscules and extraradical mycelia under drought stress highlighted the fundamental role of AMF in plant drought tolerance.

Both GintAQPF1 and GintAQPF2 have six transmembrane domains. NPK/NPA and NAA/NPA motifs exist in GintAQPF1 and GintAQPF2 (Fig. 1), respectively, which is in accordance with the fungal aquaporins (NPx and NxA) found by Pettersson *et al.* (2005). For the ar/R region, there are obvious alterations in both GintAQPF1 and GintAQPF2 from the two model

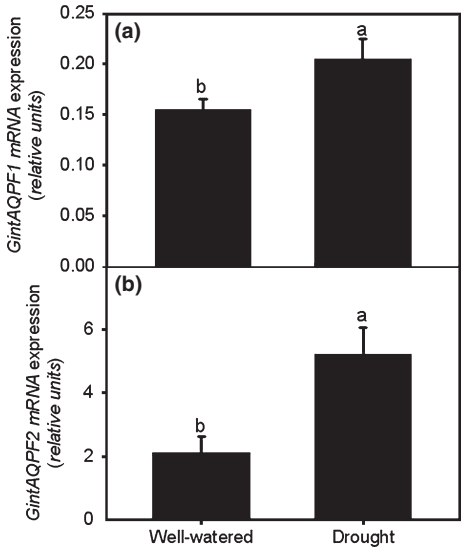

Fig. 10 Effects of drought stress on the expression of aquaporin genes, *GintAQPF1* (a) and *GintAQPF2* (b), in extraradical mycelia of *Glomus intraradices*. Different letters above the columns indicate significant differences (*t*-test, $P < 0.05$) between water treatments. The error bars represent SD.

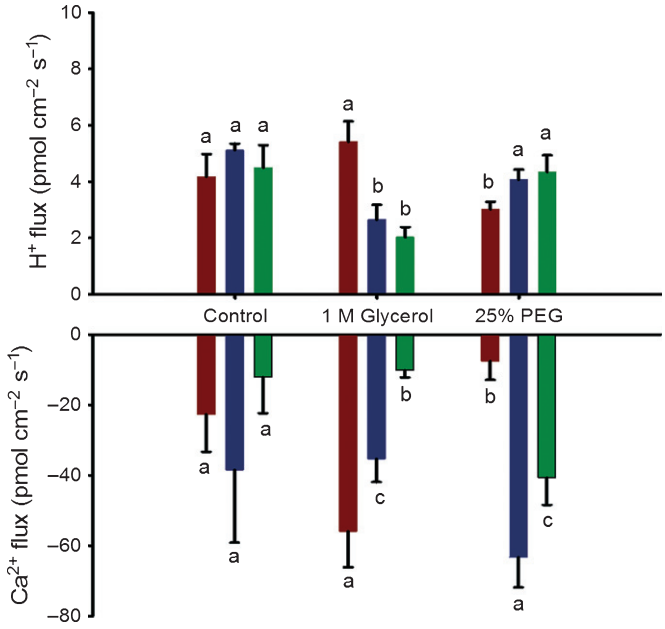

Fig. 11 Changes in extracellular Ca^{2+} influx and intracellular H^+ efflux across transformed *Pichia pastoris* Gs 115 cells in response to glycerol and polyethylene glycol (PEG) treatments. Different letters above the columns indicate significant differences ($P < 0.05$) between different cell groups under the same osmotic treatment. Empty Vector, red bars; *GintAQPF1*, blue bars; *GintAQPF2*, green bars. The error bars represent SD.

aquaporins, AQP1 (Sui *et al.*, 2001) and GlpF (Fu *et al.*, 2000). We did not identify whether the changes in NPA motif and ar/R region could fully explain the functional differences of the two aquaporins. Further studies should be carried out to parse the functional structure in ar/R and NPA constriction regions by mutational analysis.

In view of the technical limitations in studying AM fungal genetics, for example, the transient and unreliable transformation system as a result of the asexual reproduction and the genetically different nuclei co-existing in one AMF (Helber & Requena, 2008; Sanders & Croll, 2010), it was impossible to study the function of AMF genes in a homologous system using classical genetic approaches (Sanders & Croll, 2010). Therefore, we analyzed the functions of GintAQPF1 and GintAQPF2 by heterologous expression in *P. pastoris*, together with the *in situ* detection of net Ca^{2+} and H^+ fluxes that potentially regulate the gating/activity of aquaporins (Carvajal *et al.*, 2000; Martinez-Ballesta *et al.*, 2000; Nemeth-Cahalan & Hall, 2000; Karin *et al.*, 2004; Nyblom *et al.*, 2009) using the MIFE technique (Shabala *et al.*, 2001). By mimicking osmotic stress, we found that there were different response mechanisms between GintAQPF1 and GintAQPF2 to glycerol and PEG treatments. Aquaglyceroporins exhibit the ability to conduct glycerol to alleviate osmotic stress in yeasts (Tamas *et al.*, 1999), which was also verified by Pettersson *et al.* (2006). However, the *G. intraradices* aquaglyceroporin GintAQPF2 was sensitive to glycerol as shown by the significantly inhibited growth of GintAQPF2-transformed cells in the presence of 1 M glycerol (Fig. 6a). When the glycerol concentration was decreased to 0.5 M, the growth of GintAQPF2-transformed cells was still inhibited significantly (data not shown). Previous studies have shown that the characteristics of Ca^{2+} and H^+ flux may reflect the activities of aquaporins, as the up-regulation of aquaporin activities is associated directly with the decrease in cytoplasmic H^+ concentration and increase in cytoplasmic Ca^{2+} concentration (Verdoucq *et al.*, 2008; Nyblom *et al.*, 2009). In response to 1 M glycerol, Ca^{2+} influx and H^+ efflux across membranes of the GintAQPF2-transformed cells were inhibited significantly (Fig. 11), suggesting that glycerol actually decreased the activity of GintAQPF2. Likewise, 1 M glycerol also reduced the activity of GintAQPF1 in a heterologous experiment (Fig. 6a). The growth inhibition of the GintAQPF1-transformed cells was possibly a result of the greater water efflux from cells via GintAQPF1 caused by the high glycerol concentration. However, GintAQPF1-transformed cells showed better growth under 0.5 M than 1 M glycerol treatment (data not shown). It is an interesting finding that GintAQPF2 is sensitive to glycerol. Could it be the first aquaglyceroporin sensitive to glycerol to date? Further evidence needs to be obtained from the structural analysis of GintAQPF2, especially the ar/R region, by mutational analysis.

Both GintAQPF1 and GintAQPF2 alleviated significantly the adverse effects of PEG on yeast growth in heterologous expression experiments (Fig. 6b). Accordingly, Ca^{2+} influx and H^+ efflux across membranes of the GintAQPF1- and GintAQPF2-transformed cells were increased significantly by PEG treatment (Fig. 11), indicating that PEG actually stimulates the activity of GintAQPF1 and GintAQPF2. Higher aquaporin activities result from Ca^{2+} influx and increased cytosolic Ca^{2+} concentrations that can activate many kinase-dependent signaling cascades, including the mitogen-activated protein kinase (MAPK) cascade and certain protein kinases, when cells are exposed to osmotic stress (Benfenati *et al.*, 2011). The MAPK cascade may then initiate

gene expression and the biosynthesis of certain compatible osmolytes to aid in the resistance to osmotic stress, and protein kinases may phosphorylate aquaporins and facilitate water transport (Bray, 1997; Johansson *et al.*, 1998; Xiong *et al.*, 2002). The balance of the water potential between PEG outside the membranes and increased compatible osmolytes inside the membranes is also conducive to increasing the activities of aquaporins (Zimmerberg & Parsegian, 1986). However, as GintAQPF1 and GintAQPF2 triggered different Ca^{2+} influx across the cell membranes (Fig. 11), different Ca^{2+} signal sensor systems may exist in GintAQPF1- and GintAQPF2-transformed cells. We predicted that the putative calmodulin binding site was present in GintAQPF1, but not in GintAQPF2, which could explain the differences in sensoring of the Ca^{2+} signal between the two aquaporins. As *GintAQPF2*-transformed cells showed almost the same growth potential as *GintAQPF1*-transformed cells (Fig. 6b), further studies should be carried out to confirm the protein complex composed of the two aquaporins, and to determine whether different activities and Ca^{2+} signal sensor systems of the two aquaporins may lead to the same functions in alleviating the adverse effects of PEG. Nevertheless, the different responses of the two aquaporins to glycerol and PEG should be further studied to reveal the regulation mechanisms of aquaporin activities by osmolytes of different size.

As shown in Fig. 3, GintAQPF2 was clearly localized to both plasma and intracellular membranes of yeast cells. The multiple localization of GintAQPF2, compared with GintAQPF1, could possibly lead to the higher tolerance of transformed yeast cells to PEG stress (Fig. 6b) by means of the regulation of water transport through the extracellular matrix, cytoplasm and cell organelles. In comparison with GintAQPF1, GintAQPF2-transformed cells also exhibited a decrease in cell volume on hyperosmotic shock and faster protoplast bursting on hypo-osmotic shock (Figs 4, 5). We can therefore deduce that GintAQPF2 exhibits a higher capacity to transport water and may more efficiently aid cells in their resistance to osmotic stress. However, further evidence is still necessary to identify GintAQPF2 in intracellular membranes.

As a result of the definite functions of AM fungal aquaporins in coping with PEG stress, and the water transport mediated by the two aquaporins (Figs 4, 5), it is reasonable to deduce that, when drought is imposed on AM fungal mycelium, the expression of *GintAQPF1* and *GintAQPF2* will be induced and Ca^{2+} influx will be stimulated. Bonfante & Genre (2010) stated that there was signal exchange between plants and AMF. When AM plants were exposed to drought, stress signal transduction between the plant and AMF partner occurred and there was enhanced plant dependence on AMF, as shown by the increased root colonization rate (Table 2). The increase in plant dependence on AMF and the greater expression of *GintAQPF1* and *GintAQPF2* in colonized maize roots (Fig. 8), especially in arbuscule-containing cortical cells (Fig. 9), guarantee greater water delivery from AMF to plants under drought stress. Based on the heterologous expression experiment (Figs 4, 5, 6b), GintAQPF2 can contribute more water to host plants. The two aquaporins may possibly even be located at the plant–fungus interface, based on the localization of the aquaporins at the plasma membrane of *P. pastoris* (Fig. 3) and, specifically, the strong gene expression in arbuscule-enriched cortical cells (Fig. 7).

Our data showed that the expression of *GintAQPF1* and *GintAQPF2* in extraradical mycelia in HC was higher under drought than under well-watered conditions (Fig. 10). The up-regulation of *GintAQPF1* and *GintAQPF2* in extraradical mycelia resulted in water transport from soil to hyphae, and the resulting increase in cytosolic Ca^{2+} concentration may promote the biosynthesis of compatible osmolytes to help AMF to resist drought stress. The increase in compatible osmolytes may further maintain the water potential difference between the outside and inside of AM fungal cells to enhance water uptake by hyphae from soil (Allen, 2007; Egerton-Warburton *et al.*, 2007). In addition, drought significantly promoted hyphal growth (Table 2), which could enlarge the water absorption area. Furthermore, to reduce drought stress, AMF may not only transport more water to the plant by regulating their own aquaporin activities, but may also regulate the expression of plant aquaporin genes to improve plant water relations. Ruiz-Lozano *et al.* (2009) showed that, under drought stress, *G. intraradices* enhanced significantly the expression of three PIP genes and protein accumulation in colonized maize roots, which resulted in a significant increase in the root relative water content. Thus, AMF may simultaneously regulate the expression and activity of aquaporin in host plants and in fungi themselves to enhance plant tolerance to drought.

In conclusion, we have identified two functional aquaporin genes from the AMF *G. intraradices*, and have examined gene expression in both extraradical mycelia and arbuscule-enriched cortical cells under drought stress. This research provides molecular evidence for AM fungal transport of water to plants under osmotic stress, and leads to a deeper insight into the role of AMF in enhancing plant drought tolerance. In future studies, the localization of *GintAQPF1* and *GintAQPF2* in fungal structures, the relationship between alterations in NPA and the ar/R region and protein function, and the response mechanisms of aquaporins to different osmolytes based on their protein structure should be addressed.

Acknowledgements

This study was financially supported by the Knowledge Innovation Program of the Chinese Academy of Sciences (Project no. KZCX2-YW-BR-17) and the State Key Laboratory of Urban and Regional Ecology (Project no. SKLURE2008-1-03).

References

Agre P, King LS, Yasui M, Guggino WB, Ottersen OP, Fujiyoshi Y, Engel A, Nielsen S. 2002. Aquaporin water channels–from atomic structure to clinical medicine. *The Journal of Physiology* **542**: 3–16.

Allen MF. 2007. Mycorrhizal fungi: highways for water and nutrients in arid soils. *Vadose Zone Journal* **6**: 291–297.

Allen MF. 2009. Bidirectional water flows through the soil–fungal–plant mycorrhizal continuum. *New Phytologist* **182**: 290–293.

Altschul SF, Gish W, Miller W, Myers EW, Lipman DJ. 1990. Basic local alignment search tool. *Journal of Molecular Biology* **215**: 403–410.

Aroca R, Bago A, Sutka M, Antonio PJ, Cano C, Amodeo G, Ruiz-Lozano JM. 2009. Expression analysis of the first arbuscular mycorrhizal fungi aquaporin described reveals concerted gene expression between salt-stressed and nonstressed mycelium. *Molecular Plant–Microbe Interactions* **22**: 1169–1178.

Aroca R, Ruiz-Lozano JM. 2009. Induction of plant tolerance to semi-arid environments by beneficial soil microorganisms – a review. *Sustainable Agriculture Reviews* **2**: 121–135.

Aroca R, Vernieri P, Ruiz-Lozano JM. 2008. Mycorrhizal and non-mycorrhizal *Lactuca sativa* plants exhibit contrasting responses to exogenous ABA during drought stress and recovery. *Journal of Experimental Biology* **59**: 2029–2041.

Augé RM. 2001. Water relations, drought and vesicular–arbuscular mycorrhizal symbiosis. *Mycorrhiza* **11**: 3–42.

Bécard G, Fortin J. 1988. Early events of vesicular–arbuscular mycorrhiza formation on Ri T-DNA transformed roots. *New Phytologist* **108**: 211–218.

Beitz E. 2005. Aquaporins from pathogenic protozoan parasites: structure, function and potential for chemotherapy. *Biology of the Cell* **97**: 373–383.

Benfenati V, Caprini M, Dovizio M, Mylonakou MN, Ferroni S, Ottersen OP, Amiry-Moghaddam M. 2011. An aquaporin-4/transient receptor potential vanilloid 4 (AQP4/TRPV4) complex is essential for cell-volume control in astrocytes. *Proceedings of the National Academy of Sciences, USA* **108**: 2563–2568.

Biermann B, Linderman RG. 1981. Quantifying vercular–arbuscular mycorrhizas: a proposed method towards standardization. *New Phytologist* **87**: 63–67.

Bonfante P, Genre A. 2010. Mechanisms underlying beneficial plant–fungus interactions in mycorrhizal symbiosis. *Nature Communications* **1**: 48.

Bray EA. 1997. Plant responses to water deficit. *Trends in Plant Science* **2**: 48–56.

Calamita G, Bishai WR, Preston GM, Guggino WB, Agre P. 1995. Molecular cloning and characterization of AqpZ, a water channel from *Escherichia coli*. *Journal of Biological Chemistry* **270**: 29063–29066.

Carvajal M, Cerda A, Martinez V. 2000. Does calcium ameliorate the negative effect of NaCl on melon root water transport by regulating aquaporin activity? *New Phytologist* **145**: 439–447.

Compant S, van der Heijden MGA, Sessitsch A. 2010. Climate change effects on beneficial plant–microorganism interactions. *FEMS Microbiology Ecology* **73**: 197–214.

Danielson J, Johanson U. 2008. Unexpected complexity of the aquaporin gene family in the moss *Physcomitrella patens*. *BMC Plant Biology* **8**: 45.

Dietz S, von Bulow J, Beitz E, Nehls U. 2011. The aquaporin gene family of the ectomycorrhizal fungus *Laccaria bicolor*: lessons for symbiotic functions. *New Phytologist* **190**: 927–940.

Duncan DB. 1955. Multiple range and multiple F-tests. *Biometrics* **11**: 1–42.

Egerton-Warburton LM, Querejeta JI, Allen MF. 2007. Common mycorrhizal networks provide a potential pathway for the transfer of hydraulically lifted water between plants. *Journal of Experimental Biology* **58**: 1473–1483.

Finlay RD. 2008. Ecological aspects of mycorrhizal symbiosis: with special emphasis on the functional diversity of interactions involving the extraradical mycelium. *Journal of Experimental Biology* **59**: 1115–1126.

Fu D, Libson A, Miercke LJW, Weitzman C, Nollert P, Krucinski J, Stroud RM. 2000. Structure of a glycerol conducting channel and the basis for its selectivity. *Science* **290**: 481–486.

Gabor ET, Istvan S. 2001. The HMMTOP transmembrane topology prediction server. *Bioinformatics Applications Note* **17**: 849–850.

Gomez SK, Javot H, Deewatthanawong P, Torres-Jerez I, Tang YH, Blancaflor EB, Udvardi MK, Harrison MJ. 2009. *Medicago truncatula* and *Glomus intraradices* gene expression in cortical cells harboring arbuscules in the arbuscular mycorrhizal symbiosis. *BMC Plant Biology* **9**: 10.

Gónzalez-Guerrero M, Azcón-Aguilar C, Mooney M, Valderas A, MacDiarmid CW, Eide DJ, Ferrol N. 2005. Characterization of a *Glomus intraradices* gene encoding a putative Zn transporter of the cation diffusion facilitator family. *Fungal Genetics and Biology* **42**: 130–140.

Gupta AB, Sankararamakrishnan R. 2009. Genome-wide analysis of major intrinsic proteins in the tree plant *Populus trichocarpa*: characterization of XIP subfamily of aquaporins from evolutionary perspective. *BMC Plant Biology* **9**: 134.

Helber N, Requena N. 2008. Expression of the fluorescence markers DsRed and GFP fused to a nuclear localization signal in the arbuscular mycorrhizal fungus *Glomus intraradices*. *New Phytologist* **177**: 537–548.

Heller KB, Lin EC, Wilson TH. 1980. Substrate specificity and transport properties of the glycerol facilitator of *Escherichia coli*. *Journal of Bacteriology* **144**: 274–278.

Herrera-Medina MJ, Steinkellner S, Vierheilig H, Ocampo Bote JA, García Garrido JM. 2007. Abscisic acid determines arbuscule development and functionality in tomato arbuscular mycorrhiza. *New Phytologist* **175**: 554–564.

Ian SW, Daniel MR. 2004. Homology modeling of representative subfamilies of *Arabidopsis* major intrinsic proteins. Classification based on the aromatic/arginine selectivity filter. *Plant Physiology* **135**: 1059–1068.

Ito Y, Katsura K, Maruyama K, Taji T, Kobayashi M, Seki M, Shinozaki K, Yamaguchi-Shinozaki K. 2006. Functional analysis of rice DREB1/CBF-type transcription factors involved in cold-responsive gene expression in transgenic rice. *Plant and Cell Physiology* **47**: 141–153.

Jahromi F, Aroca R, Porcel R, Ruiz-Lozano JM. 2008. Influence of salinity on the *in vitro* development of *Glomus intraradices* and on the *in vivo* physiological and molecular responses of mycorrhizal lettuce plants. *Microbial Ecology* **55**: 45–53.

Jakobsen I, Abbott LK, Robson AD. 1992. External hyphae of vesicular–arbuscular mycorrhizal fungi associated with *Trifolium subterraneum*. 1: spread of hyphae and phosphorus inflow into roots. *New Phytologist* **120**: 371–380.

Johansson I, Karlsson M, Shukla VK, Chrispeels MJ, Larsson C, Kjellbom P. 1998. Water transport activity of the plasma membrane aquaporin PM28A is regulated by phosphorylation. *Plant Cell* **10**: 451–459.

Karin L, Nemeth-Cahalan KL, Kalman K, Hall JE. 2004. Molecular basis of pH and Ca^{2+} regulation of aquaporin water permeability. *Journal of General Physiology* **123**: 573–580.

King LS, Kozono D, Agre P. 2004. From structure to disease: the evolving tale of aquaporin biology. *Nature Reviews Molecular Cell Biology* **5**: 687–698.

Krüger M, Krüger C, Walker C, Stockinger H, Schüssler A. 2011. Phylogenetic reference data for systematics and phylotaxonomy of arbuscular mycorrhizal fungi from phylum to species level. *New Phytologist* **193**: 970–984.

Laizé V, Tacnet F, Ripoche P, Hohmann S. 2000. Polymorphism of *Saccharomyces cerevisiae* aquaporins. *Yeast* **16**: 897–903.

Martinez-Ballesta MDC, Martinez V, Carvajal M. 2000. Regulation of water channel activity in whole roots and in protoplasts from roots of melon plants grown under saline conditions. *Australian Journal of Plant Physiology* **27**: 685–691.

Maurel C, Verdoucq L, Luu DT, Santoni V. 2008. Plant aquaporins: membrane channels with multiple integrated functions. *Annual Review of Plant Biology* **59**: 595–624.

Nemeth-Cahalan KL, Hall JE. 2000. pH and calcium regulate the water permeability of aquaporin 0. *Journal of Biological Chemistry* **275**: 6777–6782.

Nyblom M, Frick A, Wang Y, Ekvall M, Hallgren K, Hedfalk K, Neutze R, Tajkhorshid E, Törnroth-Horsefield S. 2009. Structural and functional analysis of SoPIP2;1 mutants adds insight into plant aquaporin gating. *Journal of Molecular Biology* **387**: 653–668.

Oliveira R, Lages F, Silva GM, Lucas C. 2003. Fps1p channel is the mediator of the major part of glycerol passive diffusion in *Saccharomyces cerevisiae*: artefacts and re-definitions. *Biochimica et Biophysica Acta* **1613**: 57–71.

Peng Y, Lin W, Cai W, Arora R. 2007. Overexpression of a *Panax ginseng* tonoplast aquaporin alters salt tolerance, drought tolerance and cold acclimation ability in transgenic *Arabidopsis* plants. *Planta* **226**: 729–740.

Pettersson N, Filipsson C, Becit E, Brive L, Hohmann S. 2005. Aquaporins in yeasts and filamentous fungi. *Biology of the Cell* **97**: 487–500.

Pettersson N, Hagstrom J, Bill RM, Hohmann S. 2006. Expression of heterologous aquaporins for functional analysis in *Saccharomyces cerevisiae*. *Current Genetics* **50**: 247–255.

Pfaffl MW. 2001. A new mathematical model for relative quantification in real-time RT-PCR. *Nucleic Acids Research* **29**: 45.

Phillips JM, Hayman DS. 1970. Improved procedure of clearing roots and staining parasitic and vesicular–arbuscular mycorrhizal fungi for rapid assessment of infection. *Transactions of the British Mycological Society* **55**: 159–161.

Porcel R, Aroca R, Azcon R, Ruiz-Lozano JM. 2006. PIP aquaporin gene expression in arbuscular mycorrhizal *Glycine max* and *Lactuca sativa* plants in relation to drought stress tolerance. *Plant Molecular Biology* **60**: 389–404.

Porcel R, Azcon R, Ruiz-Lozano JM. 2004. Evaluation of the role of genes encoding for Δ^1-pyrroline-5-carboxylate synthetase (P5CS) during drought stress in arbuscular mycorrhizal *Glycine max* and *Lactuca sativa* plants. *Physiological and Molecular Plant Pathology* **65**: 211–221.

Prudent S, Marty F, Charbonnier M. 2005. The yeast osmosensitive mutant *fps1*Δ transformed by the cauliflower BobTIP1;1 aquaporin withstand a hypo-osmotic shock. *FEBS Letters* **579**: 3872–3880.

Querejeta JI, Egerton-Warburton LM, Allen MF. 2009. Topographic position modulates the mycorrhizal response of oak trees to interannual rainfall variability. *Ecology* **90**: 649–662.

Ruiz-Lozano JM. 2003. Arbuscular mycorrhizal symbiosis and alleviation of osmotic stress. New perspectives for molecular studies. *Mycorrhiza* **13**: 309–317.

Ruiz-Lozano JM, Azcon R. 1997. Effect of calcium application on the tolerance of mycorrhizal lettuce plants to polyethylene glycol-induced water stress. *Symbiosis* **23**: 9–22.

Ruiz-Lozano JM, del Mar Alguacil M, Barzana G, Vernieri P, Aroca R. 2009. Exogenous ABA accentuates the differences in root hydraulic properties between mycorrhizal and non mycorrhizal maize plants through regulation of PIP aquaporins. *Plant Molecular Biology* **70**: 565–579.

Ruiz-Lozano JM, Porcel R, Aroca R. 2006. Does the enhanced tolerance of arbuscular mycorrhizal plants to water deficit involve modulation of drought-induced plant genes? *New Phytologist* **171**: 693–698.

Ruíz-Sánchez M, Armada E, Muñoz Y, de Salamone IEG, Aroca R, Ruíz-Lozano JM, Azcón R. 2011. *Azospirillum* and arbuscular mycorrhizal colonization enhance rice growth and physiological traits under well-watered and drought conditions. *Journal of Plant Physiology* **168**: 1031–1037.

Sade N, Vinocur BJ, Diber A, Shatil A, Ronen G, Nissan H, Wallach R, Karchi H, Moshelion M. 2009. Improving plant stress tolerance and yield production: is the tonoplast aquaporin SlTIP2;2 a key to isohydric to anisohydric conversion? *New Phytologist* **181**: 651–661.

Sanders IR, Croll D. 2010. Arbuscular mycorrhiza: the challenge to understand the genetics of the fungal partner. *Annual Review of Genetics* **44**: 271–292.

Shabala L, Ross T, McMeekin T, Shabala S. 2006. Non-invasive microelectrode ion flux measurements to study adaptive responses of microorganisms to the environment. *FEMS Microbiology Review* **30**: 472–486.

Shabala L, Ross T, Newman I, McMeekin T, Shabala S. 2001. Measurements of net fluxes and extracellular changes of H^+, Ca^{2+}, K^+, and NH_4^+ in *Escherichia coli* using ion-selective microelectrodes. *Journal of Microbiological Methods* **46**: 119–129.

Sui H, Han BG, Lee JK, Walian P, Jap BK. 2001. Structural basis of water specific transport through the AQP1 water channel. *Nature* **414**: 872–878.

Tamas MJ, Luyten K, Sutherland FC, Hernandez A, Albertyn J, Valadi H, Li H, Prior BA, Kilian SG, Ramos J. 1999. Fps1p controls the accumulation and release of the compatible solute glycerol in yeast osmoregulation. *Molecular Microbiology* **31**: 1087–1104.

Tamura K, Dudley J, Nei M, Kumar S. 2007. MEGA4: molecular evolutionary genetics analysis (MEGA) software version 4.0. *Molecular Biology and Evolution* **24**: 1596–1599.

Tanghe A, Van Dijck P, Thevelein JM. 2006. Why do microorganisms have aquaporins? *Trends in Microbiology* **14**: 78–85.

Tisserant E, Kohler A, Dozolme-Seddas P, Balestrini R, Benabdellah K, Colard A, Croll D, Da Silva C, Gomez SK, Koul R *et al.* 2012. The transcriptome of the arbuscular mycorrhizal fungus *Glomus intraradices* (DAOM 197198) reveals functional tradeoffs in an obligate symbiont. *New Phytologist* **193**: 755–769.

Verdoucq L, Grondin A, Maurel C. 2008. Structure–function analysis of plant aquaporin at PIP2;1 gating by divalent cations and protons. *Biochemical Journal* **415**: 409–416.

Waterham HR, Digan ME, Koutz PJ, Lair SV, Cregg JM. 1997. Isolation of the *Pichia pastoris* glyceraldehyde-3-phosphate dehydrogenase gene and regulation and use of its promoter. *Gene* **186**: 37–44.

Xiong LM, Schumaker KS, Zhu JK. 2002. Cell signaling during cold, drought, and salt stress. *Plant Cell* **14**: 165–183.

Yu Q, Hu Y, Li J, Wu Q, Lin Z. 2005. Sense and antisense expression of plasma membrane aquaporin BnPIP1 from *Brassica napus* in tobacco and its effects on plant drought resistance. *Plant Science* **169**: 647–656.

Zimmerberg J, Parsegian VA. 1986. Polymer inaccessible volume changes during opening and closing of a voltage-dependent ionic channel. *Nature* **323**: 36–39.